Article

A Study on Efficient Technique for Generating Vertex-based Topological Characterization of Boric Acid 2D Structure

Sahaya Vijay Jeyaraj and Roy Santiago*

Cite This: *ACS Omega* 2023, 8, 23089−23097

Read Online

| ACCESS | | Metrics & More | | Article Recommendations |

ABSTRACT: The computational technique called the cut method is used to predict the natural behaviors among the chemical network's physicochemical characteristics, known as topological indices. Distance-based indices are used to describe the physical density of chemical networks. In this paper, we have done analytical computation results for the vertex-distance-based and vertex-degree-based indices for boric acid hydrogen-bonded 2D lattice sheet. Boric acid is an inorganic compound with low toxicity when applied to the skin or eaten. A graphical representation is used to explain a thorough comparison of the computed topological indices of hydrogen-bonded 2D lattice sheets of boric acid.
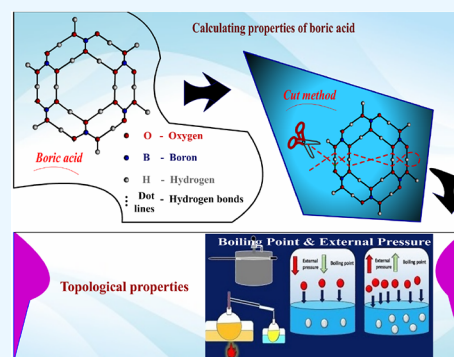
1. INTRODUCTION

Chemical graph theory is a branch of mathematical chemistry that uses graph theory to study the topology of chemical compounds. In mathematical chemistry, chemical graph theory has several applications. The vertices and edges of a chemical graph represent a molecular structure's atoms and bonds, respectively. Graph theory is essential for predicting chemical structure using numerical quantities (that is, topological indices (TI)).[1]

In this paper, we have done analytical computation for boric acid structure. Chemical formula H_3BO_3 or $B(OH)_3$ for boric acid, which is an inorganic compound for cleaning and preserving food, also known as orthoboric acid, boracic acid, hydrogen borate, and acidum boricum, has been used since ancient Greece.[2,3] This substance is used for various things, including producing glass and fiberglass for LCD flat-panel displays, jewelry, additives in nuclear reactor coolants, buffers against rising pH in swimming pools, and lubricants and flame retardants. The applications of boric acid are critical in the fields of inorganic chemistry.[2,3] The temperature has a significant impact on the solubility of the molecule. Boric acid is a soluble neutron absorber, soluble poison, or chemical shim dissolved in the reactor coolant to control neutron reactivity in the core.[4] The high boron level indicates the start of a fuel cycle and compensates for the core's excess reactivity.[5] Throughout the fuel cycle, the amount is reduced due to fuel burn-up, altering core reactivity, temperature, and the accumulation of other poisons like xenon and samarium.[6] In 1702, Wilhelm Hornberg created the first crystals of boric acid. He named it as sal sedativum Hombergi (sedative salt of Hornberg). Planar BO_3
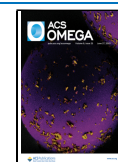
units are connected by hydrogen bonds in a polymeric layer structure in boric acid (see Figure 1a). Boric acid is considered as a boric acid 2D sheet (see Figure 1b) in this study.[7]

Topological indices are numerical values associated with a graph that describes the graph's underlying connectivity.[8] The concept of topological index arose due to Wiener's pioneering work on paraffin boiling points and other physicochemical properties of chemical substances. Their networks and the underlying molecular topology strongly influence the chemical and biological characteristics of polycyclic aromatic structures. For predicting attributes of polycyclic rosette layers and related graphs from molecular structures, quantitative structure−activity relationship (QSAR) and quantitative structure−property relationship (QSPR) approaches have been developed.[9−38] Because of their widespread use in the petroleum, chemical, and pharmaceutical sectors, they are of great interest in the chemical field. As a result, their toxicity, carcinogenicity, and cutaneous penetrations have all gotten a lot of press.[13−23] Using QSAR and QSPR approaches, many of these compounds' observable features and toxicity potentials may be predicted from their structures.[14−31] Furthermore, dermal penetration is closely related to the shape and hydrophobicity of molecules. Specific aspects of polycyclic aromatic compounds appear more

O - Oxygen
B - Boron
H - Hydrogen
Dot lines - Hydrogen bonds

(a) Structure of BO_3; the dotted lines represent hydrogen bond

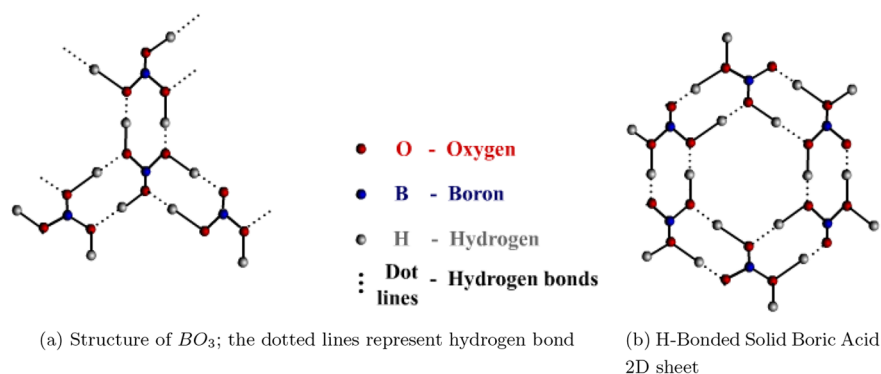(b) H-Bonded Solid Boric Acid 2D sheet

Figure 1. Boric acid structures.

strongly correlated with their topological connectivity.[14−23] For the pioneering works, some topological descriptors have been developed for chemical molecular graphs like Wiener[37] and Randić[38] on both vertex-distance-based and degree-based topological indices. To assess uniqueness when examining chemical information, they offered topological indices that were blatantly biased. In chemistry and nanotechnology, numerous graphical features are helpful. Consequently, computing topological invariants is one of the valuable fields of graphical study.

The review of experimental and theoretical literature presented above reveals a clear and importance of proper analytical computation for the various topological descriptors of hydrogen-bonded solid boric acid. We have developed the graph theoretical techniques based on cut method to derive exact analytical formula for complicated rosette layers of solid boric acid structures as a function of two-dimensional characteristics that characterize these structures in the broadest sense. Section 2 tells about the structure's growth of hydrogen-bonded solid boric acid 2D lattice sheet. Section 3 covers the fundamental terminologies as well as the analytical computation method for distance-based topological indices. In Section 4.1, we look at distance-based topological indices for solid boric acid 2D sheet systems, and in Section 4.2, we look at degree-based topological indices. Finally, in Section 4.3, we show highly correlated indices which are most helpful for getting physicochemical properties.

2. HYDROGEN BONDED BORIC ACID 2D LATTICE SHEET

Wilhelm Homberg created the first crystals of boric acid for 1702. Due to its reducing nature and antibacterial properties, boric acid (also known as sodium tetraborate) has been used as a preservative for crustacean, especially shrimps, to prevent enzymatic darkening that degrades the quality of seafood after fishing. Boric acid is considered a hydrogen-bonded solid boric acid 2D sheet (BA-2D) in Figure 1b. BA-2D structures have multiple cycles, so this structure is considered as rosette layer.

Atoms and hydrogen bonds are called vertices and edges in this context. The anionic rosette layers[39] were developed from BA-2D. In this paper, we derived bulk boric acid 2D lattice sheet[40] (BAL-2D(m, n)) like anionic rosette layers. BAL-2D(m, n) is parallelogram-like h-bonded solid boric acid 2D lattice sheet (see Figure 2).

3. COMPUTATIONAL METHODS

A simple and connected graph G is a collection of vertices $V(G)$ and edges $E(G)$ without loops and multiple edges. Let $|V(G)| =$
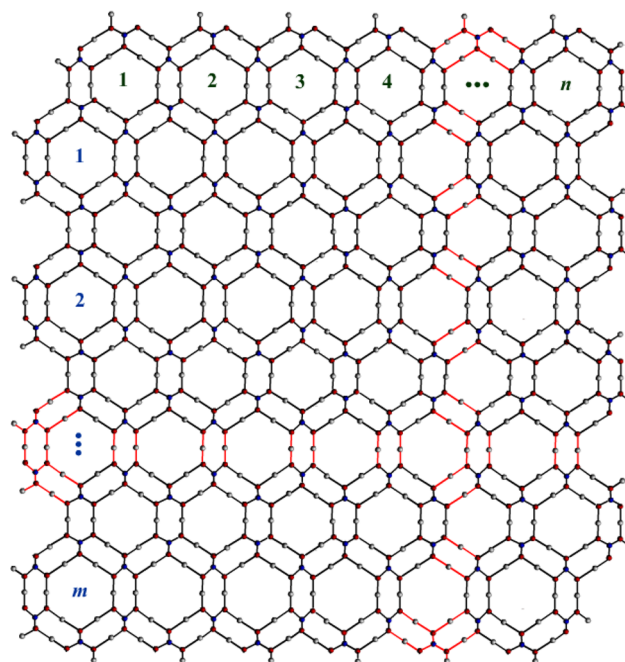

Figure 2. Boric acid 2D graphene sheet BAL-2D(m, n).

M and $|E(G)| = N$, respectively. The degree of any vertex v of G represented by $d_G(v)$ is the number of edges incident to v. The length of a shortest path between the two vertices u and v of G is denoted by $d_G(u, v)$. For any two edges $e = uv$ and $f = ab$ in $E(G)$, the length of a shortest path between the two edges e and f is denoted by $d_G(e, f)$. We define $d_G(u, f) = min\{d_G(u, a), d_G(u, b)\}$. In this paper, we use $d(v)$ and $d(u, v)$ for $d_G(v)$ and $d_G(u, v)$.

Let $e = uv$, we define

$$n_u(e) = |\{a \in V(G): d(u, a) < d(v, a)\}|$$

$$n_v(e) = |\{a \in V(G): d(v, a) < d(u, a)\}|$$

Different types of vertex-version distance based TIs which are used in the paper are given in Table 1.

The Θ*-class or cut method is a perfect tool for computing topological descriptors of complex structures by splitting the related graph into smaller parts and arranging the descriptors of the fragments to get the property of the entire network. The efficiency of Θ*-class is in obtaining distance-based topological indices of families of chemical graphs. The class of partial cubes is the most popular class of molecular structures for which the

Table 1. Different Types of Vertex-Version of Distance Based TI's

TI's	mathematical formula
Wiener[37]	$WI_v(G) = \sum_{\{u,v\} \subseteq V(G)} d(u, v)$
Vertex-Szeged[47]	$Sz_v(G) = \sum_{e=uv \in E(G)} n_u(e)n_v(e)$
Vertex-Padmakar-Ivan[48]	$PI_v(G) = \sum_{e=uv \in E(G)} n_u(e) + n_v(e)$

cut method has proven particularly beneficial. The cut method was first developed on benzenoid structures.[41]

We recall Djoković−Winkler relation and convex subgraph for the cut method. Isometric subgraphs of graphs are those in which the length of the shortest path between any two vertices of the subgraph is calculated in the subgraph or the whole graph. The Djoković−Winkler relation Θ is characterized on $E(G)$ as follows: if $g = ab \in E(G)$ and $h = uv \in E(G)$, then $g\Theta h$ if $d_G(a, u) + d_G(b, v) \neq d_G(a, v) + d_G(b, u)$.[42−46]

The cut method can be used to create algorithms for computing topological indices based on distance.

Theorem 3.1.[49] Let G_1 and G_2 be graphs with Θ^*-classes F_i where $1 \leq i \leq k$. Then $G_1 - F_i$ has exactly two components A and B and $G_2 - F_i$ has more than two components $(A, B, C, \cdots)$ are convex. Let $n_1(A)$ and $n_1(B)$ are number of vertices of two components A and B respectively. Let $|C|$ denote the total number of all compounds containing only isolated vertices in $G_2 - F_i$ and the length of the shortest path between two isolated vertices a and b of G_2 is denoted by $d_{G_2}(a, b)$. Here instead of $d_{G_2}(a, b)$, we use $d(a, b)$. Then

For $G_1 - F_i$,

(i) $WI_v(G_1) = \sum_{i=1}^{k} n_1(F_i)n_2(F_i)$,

(ii) $Sz_v(G_1) = \sum_{i=1}^{k} |F_i|n_1(F_i)n_2(F_i)$,

(iii) $PI_v(G_1) = \sum_{i=1}^{k} |F_i|(n_1(F_i) + n_2(F_i))$ and

For $G_2 - F_i$,

(i) $WI_v(G_2) = \sum_{i=1}^{k} 2n_1(F_i)n_2(F_i) + \sum_{i=1}^{k} |C|n_1(F_i) + |C|n_2(F_i)$,
$+ \sum_{i=1}^{k} d(a, b)$

(ii) $Sz_v(G_2) = \sum_{i=1}^{k} |F_i|n_1(F_i)n_2(F_i)$,

(iii) $PI_v(G_2) = \sum_{i=1}^{k} |F_i|(n_1(F_i) + n_2(F_i))$.

4. RESULTS AND DISCUSSION

4.1. Vertex-Version of Distance-Based Topological Indices. In this section, we obtain some vertex-version of
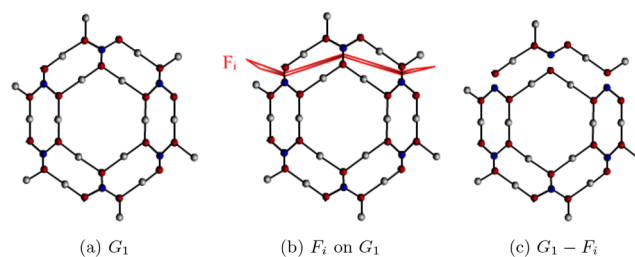
Table 2. Notations of Θ^*-Classes

| Θ^*-classes	notations		directions	
horizontal	H_{1i}, H_{2i}	H_{-1i}, H_{-2i}	North	South
obtuse	O_{1i}, O_{2i}	O_{-1i}, O_{-2i}	Northeast	Southwest
acute	A_{1i}, A_{2i}	A_{-1i}, A_{-2i}	Northwest	Southeast

distance-based topological descriptors for hydrogen-bonded boric acid 2D sheet structure. Table 2 shows notations of Θ^*-classes depicted in Figures 3 and 4. We used Matlab software for analytical computation and also used Flash8 software for constructing all Figures in this study.

Let,

(i) $WI_v(F) = n_1(F)n_2(F)$

(ii) $Sz_v(F) = |F|[n_1(F)n_2(F)]$

Figure 3. Illustration for Θ^*-relation of G_1.

(a) G_1 (b) F_i on G_1 (c) $G_1 - F_i$
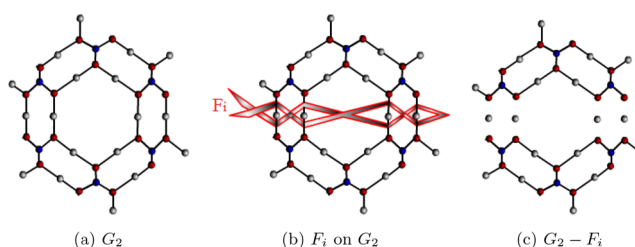
Figure 4. Illustration for Θ^*-relation G_2.

(a) G_2 (b) F_i on G_2 (c) $G_2 - F_i$

Table 3. Size of Θ^*-Classes

F_i	range	$|F_i|$
H_{1i}	$1 \leq i \leq 2m + 1$	$2m + 1$
O_{1i}	$1 \leq i \leq m + n + 1$	$m + n + 1$
A_{1i}	$1 \leq i \leq m + n$	$m + n$
P_i	$1 \leq i \leq m + n + 1$	$4m + 2n + 2$
H_{2i}	$1 \leq i \leq 2m$	$2m$
O_{2i}	$1 \leq i \leq m + n$	$m + n$
A_{2i}	$1 \leq i \leq m + n$	$m + n$
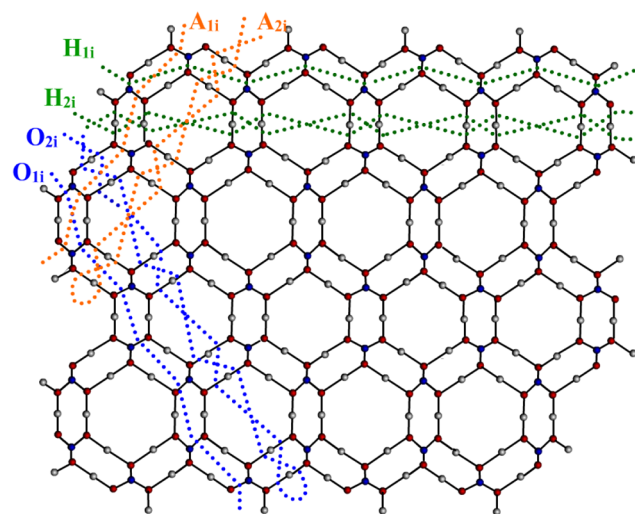
Figure 5. Types of Θ^*-classes.

(iii) $PI_v(F) = |F|[n_1(F) + n_2(F)]$, where $F = H_{1i}, O_{1i}, O_{-1i}, A_{1i}, A_{-1i}, P_i$.

and

(i) $WI_v(F) = 2n_1(F)n_2(F) + |C|n_1(F) + |C|n_2(F) + d(a, b)$

(ii) $Sz_v(F) = |F|[n_1(F)n_2(F)]$

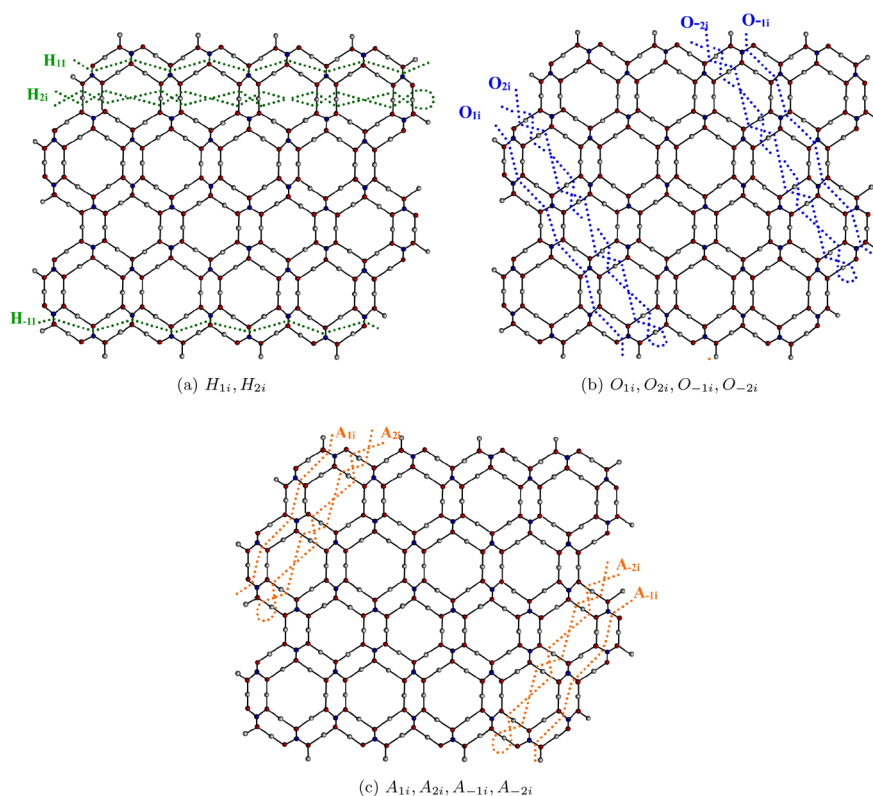(iii) $PI_v(F) = |F|[n_1(F) + n_2(F)]$, where $F = H_{2i}, O_{2i}, O_{-2i}, A_{2i}, A_{-2i}$.

(a) H_{1i}, H_{2i}

(b) $O_{1i}, O_{2i}, O_{-1i}, O_{-2i}$

(c) $A_{1i}, A_{2i}, A_{-1i}, A_{-2i}$

Figure 6. (a) Horizontal cuts, (b) obtuse cuts, and (c) acute cuts.

Table 4. Cardinality of Partitions of Θ*-Classes

cases	F_i	range	$|F_i|$
if $m \leq n$	H_{1i}	$1 \leq i \leq 2$	$2n + i$
		$3 \leq i \leq 2m$	$2n + 2$
		$2m + 1 \leq i \leq 2m + 1$	$2n + i$
if $m < n$	O_{1i}	$1 \leq i \leq m$	$4i - 1$
		$m + 1 \leq i \leq m + 1$	$4m + 1$
		$m + 2 \leq i \leq n$	$4m + 2$
if $m = n$	O_{1i}	$1 \leq i \leq m$	$4i - 1$
		$m + 1 \leq i \leq m + 1$	$4m$
if $m \leq n$	A_{1i}	$1 \leq i \leq m$	$4i + 1$
		$m + 1 \leq i \leq n$	$4m + 2$
	P_i	$1 \leq i \leq 4m + 2n + 2$	1
	H_{2i}	$1 \leq i \leq 2m$	
	O_{2i}	$1 \leq i \leq m$	
		$m + 1 \leq i \leq n$	
	A_{2i}	$1 \leq i \leq m - 1$	
		$m \leq i \leq n$	

Theorem 4.1. Let G be a Hydrogen bonded boric acid 2D sheet lattice structure BAL-2D(m, n).

If $m < n$, then

1.
$$WI_v(G) = -\frac{1}{5}(392m^5 - 1960m^4n - 980m^4 - 3920m^3n^2$$
$$- 11760m^3n - 4990m^3 - 3920m^2n^3$$
$$- 17640m^2n^2 - 20870m^2n - 2765m^2 - 3920mn^3 - 8630mn^2$$
$$- 6010mn + 273m - 980n^3$$
$$- 385n^2 - 165n + 90)$$

2.
$$Sz_v(G) = \frac{2}{15}(2352m^5 - 7840m^4n - 6340m^4 + 35280m^3n^3$$
$$+ 105840m^3n^2 + 98920m^3n + 23180m^3$$
$$+ 52920m^2n^3 + 105840m^2n^2 + 66820m^2n + 4285m^2$$
$$+ 24930mn^3 + 27030mn^2 + 10430mn$$
$$+ 1003m + 3675n^3 + 210n^2 - 240n - 135)$$

3. $PI_v(G) = 1008m^2n^2 + 1904m^2n + 896m^2 + 952mn^2 + 840mn - 56m + 224n^2 - 28n$

If $m = n$, then

1.
$$WI_v(G) = -\frac{1}{15}(2156m^5 - 8820m^4n - 1960m^4 - 11760m^3n^2$$
$$- 44100m^3n - 15945m^3 - 9800m^2n^3$$
$$- 47040m^2n^2 - 65065m^2n - 8195m^2 - 9800mn^3 - 22950mn^2$$
$$- 18130mn$$
$$+ 439m - 2450n^3 - 1155n^2 - 115n + 150)$$

2.
$$Sz_v(G) = -\frac{2}{15}(1960m^6 - 5880m^5n + 588m^5 - 12740m^4n$$
$$+ 5850m^4 - 31360m^3n^3 - 94080m^3n^2$$
$$- 113130m^3n - 23355m^3 - 47040m^2n^3 - 94080m^2n^2$$
$$- 70075m^2n - 3865m^2 - 21990mn^3$$
$$- 24090mn^2 - 10850mn - 1173m - 3185n^3 - 210n^2 + 170n$$
$$+ 75)$$

3. $PI_v(G) = 112m^3n + 112m^3 + 896m^2n^2 + 1904m^2n + 952m^2 + 840mn^2 + 812mn - 56m + 196n^2 - 28n.$

Proof. Let G be a Hydrogen bonded solid boric acid 2D sheet lattice structure BAL-2D with dimension (m, n). We have $M = 28m + 14n + 28mn$ and $N = 32m + n(36m + 16) - 2$.

Apply Θ*-classes F_i on G, then $|F_i|$ of H_{1i}, O_{1i}, A_{1i}, P_i, H_{2i}, O_{2i}, and A_{2i} are defined below in Table 3.

There are different set of Θ*-classes F_i for H_{1i}, O_{1i}, A_{1i}, P_i, H_{2i}, O_{2i}, and A_{2i} (see Figure 5) which divide the edge set $E(G)$ into convex cuts. The sets are $\{H_{1i}: 1 \leq i \leq 2\}$, $\{H_{1i}: 3 \leq i \leq 2m\}$, $\{H_{1(2m+1)}\}$, $\{O_{1i}: 1 \leq i \leq m\}$, $\{O_{1(m+1)}\}$, $\{O_{1i}: m + 2 \leq i \leq n\}$, $\{O_{-1(n+1)}\}$, $\{O_{-1i}: n + 2 \leq i \leq m + n + 1\}$, $\{A_{1i}: 1 \leq i \leq m\}$, $\{A_{1i}: m + 1 \leq i \leq n\}$, $\{A_{-1i}: n + 1 \leq i \leq m + n\}$, $\{P_i: 1 \leq i \leq 4m + 2n + 2\}$, $\{H_{2i}: 1 \leq i \leq 2m\}$, $\{O_{2i}: 1 \leq i \leq m\}$, $\{O_{2i}: m + 1 \leq i \leq n\}$, $\{O_{-2i}: n + 1 \leq i \leq m + n + 1\}$, $\{A_{2i}: 1 \leq i \leq m\}$, $\{A_{2i}: m + 1 \leq i \leq n\}$, and

Table 5. Computation of Partitions of Θ*-Classes

cases	F_i	range	$n_1(F_i)$	$|C|$
if $m \le n$	H_{1i}	$1 \le i \le 2$	$i(14n+12) - 7n - 10$	
		$3 \le i \le 2m$	$21n + (14n+14)(i-2) + 14$	
		$2m+1 \le i \le 2m+1$	$28m + 7n + 28mn - 2$	
if $m < n$	O_{1i}	$1 \le i \le m$	$14i^2 - 7i + 2$	
		$m+1 \le i \le m+1$	$14m^2 + 21m + 2$	
		$m+2 \le i \le n$	$14i + 28im - 12$	
if $m = n$	O_{1i}	$1 \le i \le m$	$14i^2 - 7i + 2$	
		$m+1 \le i \le m+1$	$14m^2 + 21m$	
if $m \le n$	A_{1i}	$1 \le i \le m$	$14i^2 + 7i - 5$	
		$m+1 \le i \le n$	$(28m+14)i - 14m^2 - 7m - 7$	
	P_i	$1 \le i \le 4m+2n+2$	$4m + 2n + 2$	
	H_{2i}	$1 \le i \le 2m$	$14i - n + 14in - 8$	$2n+2$
	O_{2i}	$1 \le i \le m$	$14i^2 + 5i$	$4i$
		$m+1 \le i \le n$	$i(28m+14) - 14m^2 - 9m - 8$	$4m+2$
	A_{2i}	$1 \le i \le m-1$	$14i^2 + 19i - 1$	$4i+2$
		$m \le i \le n$	$(28m+14)i - 14m^2 + 5m - 1$	$4m+2$

Table 6. Cardinality of Partitions of Θ*-Classes

cases	F_i	range	$|F_i|$
if $m > n$		$1 \le i \le 2$	$2n+i$
	H_{1i}	$3 \le i \le 2m$	$2n+2$
		$2m+1 \le i \le 2m+1$	$2n+i$
		$1 \le i \le n$	$4i-1$
	O_{1i}	$n+1 \le i \le n+1$	$4n+1$
		$n+2 \le i \le m$	$4n+4$
	A_{1i}	$1 \le i \le n$	$4i+1$
		$n+1 \le i \le m$	$4n+4$
	P_i	$1 \le i \le 4m+2n+2$	1
	H_{2i}	$1 \le i \le 2m$	
	O_{2i}	$1 \le i \le n$	
		$n+1 \le i \le m$	
	A_{2i}	$1 \le i \le n-1$	
		$n \le i \le m$	

Table 7. Computation of Partitions of Θ*-Classes

cases	F_i	range	$n_1(F_i)$	$|C|$
if $m > n$	H_{1i}	$1 \le i \le 2$	$i(14n+12) - 7n - 10$	
		$3 \le i \le 2m$	$21n + (14n+14)(i-2) + 14$	
		$2m+1 \le i \le 2m+1$	$28m + 7n + 28mn - 2$	
	O_{1i}	$1 \le i \le n$	$14i^2 - 7i + 2$	
		$n+1 \le i \le n+1$	$14n^2 + 21n + 7$	
		$n+2 \le i \le m$	$i(28n+28) - 14n^2 - 35n - 28$	
	A_{1i}	$1 \le i \le n$	$14i^2 + 7i - 5$	
		$n+1 \le i \le m$	$i(28n+28) - 14n^2 - 21n - 14$	
	P_i	$1 \le i \le 4m+2n+2$	$4m + 2n + 2$	
	H_{2i}	$1 \le i \le 2m$	$14i - n + 14in - 8$	$2n+2$
	O_{2i}	$1 \le i \le m$	$14i^2 + 5i$	$4i$
		$m+1 \le i \le n$	$i(28n+28) - 14n^2 - 23n - 15$	$4n+2$
	A_{2i}	$1 \le i \le m-1$	$14i^2 + 19i - 1$	$4i+2$
		$m \le i \le n$	$(28n+28)i - 14n^2 - 9n - 1$	$4n+2$

$\{A_{-2i}: n+1 \le i \le m+n+1\}$ (see Figure 6). We have the cardinality of partitions of Θ*-classes from below Table 4

Table 8. Vertex-Degree Based Edge Set Partition

struture	$E_{(u,v)}$	$|E_{(u,v)}|$
BAL-2D(m,n)	$(1,3)$	$4m + 2n + 2$
	$(2,2)$	$4m + 2n + 2$
	$(2,3)$	$24mn + 8n + 16m - 4$
	$(3,3)$	$12mn + 4n + 8m - 2$

From the above Table 5, $n_2(F_i) = M - n_1(F_i)$, where $F_i = H_{1i}, O_{1i}, A_{1i}, P_i$

$$n_2(F_i) = M - n_1(F_i) - |C|, \quad \text{where } F_i = H_{2i}, O_{2i}, A_{2i}$$

By symmetry, we have for $k = 1$, $n_k(A_{1i}) = n_k(A_{-1i})$, $n_k(O_{1i}) = n_k(O_{-1i})$, for $1 \le i \le m$ and $n_k(O_{2i}) = n_k(O_{-2i})$ for $1 \le i \le m$ and $n_k(A_{2i}) = n_k(A_{-2i})$ for $1 \le i \le m-1$. For $m \le n$, Define

$$X(G) = \sum_{i=1}^{2} X(H_{1i}) + \sum_{i=3}^{2m} X(H_{1i}) + X(H_{1(2m+1)})$$

$$+ 2\sum_{i=1}^{m} X(O_{1i}) + 2X(O_{1m+1}) + \sum_{i=m+2}^{n} X(O_{1i})$$

$$+ 2\sum_{i=1}^{m} X(A_{1i}) + \sum_{i=m+1}^{n} X(A_{1i}) + \sum_{i=1}^{4m+2n+2} X(P_i)$$

$$+ \sum_{i=1}^{2m} X(H_{2i}) + 2\sum_{i=1}^{m} X(O_{2i}) + \sum_{i=m+1}^{n} X(O_{2i})$$

$$+ 2\sum_{i=1}^{m-1} X(A_{2i}) + \sum_{i=m}^{n} X(A_{2i}) \quad \text{where } X$$

$$= W, Sz_v, PI_v$$

Furthermore, an analytical computation of $X(G)$ gives the result of the Theorem 4.1.

Theorem 4.2. Let G be a Hydrogen bonded boric acid 2D sheet lattice structure BAL-2D(m,n). If $m > n$, then

1.
$$WI_v(G) = \frac{2}{5}(3920m^3n^2 + 7840m^3n + 3920m^3 + 5880m^2n^2$$
$$+ 6160m^2n + 280m^2 + 980mn^4 + 3920mn^3$$
$$+ 8590mn^2 + 5210mn + 900m - 196n^5 - 490n^4 - 935n^3$$
$$- 910n^2 - 954n - 270)$$

2.
$$Sz_v(G) = \frac{2}{15}(35280m^3n^3 + 98000m^3n^2 + 90160m^3n$$
$$+ 27440m^3 + 52920m^2n^3 + 94080m^2n^2$$
$$+ 42000m^2n + 840m^2 + 3920mn^4 + 49370mn^3 + 63890mn^2$$
$$+ 24780mn + 3190m - 1568n^5$$
$$- 10260n^4 - 12625n^3 - 10695n^2 - 5127n - 1545)$$

3. $PI_v(G) = 1008m^2n^2 + 1904m^2n + 896m^2 + 952mn^2 + 840mn - 56m + 224n^2 - 28n$

Proof. Let G be a Hydrogen bonded solid boric acid 2D sheet lattice structure BAL-2D with dimension (m,n). We have M = |

Table 9. Numerical Values of Distance Based Descriptors

cases	(m, n)	(1, 2)	(2, 3)	(3, 4)	(4, 5)	(5, 6)
$m < n$	WI_v	56474	490876	2119866	6479528	16051450
	Sz_v	300086	3965356	22684050	85987492	253863550
	PI_v	15008	86716	280840	687092	1419376
	(m, n)	(1, 1)	(2, 2)	(3, 3)	(4, 4)	(5, 5)
$m = n$	WI_v	17636	233998	1220840	4166150	11099932
	Sz_v	73128	1568466	11260248	48880382	158037992
	PI_v	5740	46648	176148	471856	1035580
	(m, n)	(2, 1)	(3, 2)	(4, 3)	(5, 4)	(6, 5)
$m > n$	WI_v	84066	611356	2461326	7250028	17557834
	Sz_v	401984	4493698	24328424	89930718	261913392
	PI_v	18900	95760	296940	712152	1455300

Table 10. Numerical Values of Degree Based Descriptors

(m, n)	(1, 1)	(2, 2)	(3, 3)	(4, 4)	(5, 5)
M_1	416	1232	2432	4016	5984
M_2	518	1568	3122	5180	7742
HM	2148	6468	12852	21300	31812
AZ	693.59375	2076.59375	4116.96875	6814.71875	10169.84375
ABC	57.9682	166.9921	325.9571	534.8632	793.7104
H	32.93333333	93.33333333	180.9333333	295.7333333	437.7333333
SC	36.6589	105.1873	204.9799	336.0368	498.3578
GA	80.0392	233.2958	457.5825	752.8995	1.12E + 03
R	33.9151	95.571	184.8229	301.6706	446.1143

$V(G)| = 28m + 14n + 28mn$ and $N = |E(G)| = 32m + n(36m + 16) - 2$.

Apply Θ^*-classes F_i on G, then $|F_i|$.(Refer Theorem 4.1).

We have the cardinality of partitions of Θ^*-classes from below Table 6.

There are different set of Θ^*-classes F_i for H_{1i}, O_{1i}, A_{1i}, P_i, H_{2i}, O_{2i} and A_{2i} (see Figure 5) which divide the edge set $E(G)$ into convex cuts. The sets are $\{H_{1i}: 1 \leq i \leq 2\}$, $\{H_{1i}: 3 \leq i \leq 2m\}$, $\{H_{(2m+1)}\}$, $\{O_{1i}: 1 \leq i \leq n\}$, $\{O_{n+1}\}$, $\{O_{1i}: n + 2 \leq i \leq m\}$, $\{O_{-1i}: m + 1 \leq i \leq m + n + 1\}$, $\{A_{1i}: 1 \leq i \leq n\}$, $\{A_{1i}: n + 1 \leq i \leq m\}$, $\{A_{-1i}: m + 1 \leq i \leq m + n - 1\}$, $\{P_i: 1 \leq i \leq 4m + 2n + 2\}$, $\{H_{2i}: 1 \leq i \leq 2m\}$, $\{O_{2i}: 1 \leq i \leq n\}$, $\{O_{2i}: n + 1 \leq i \leq m\}$, $\{O_{-2i}: m + 1 \leq i \leq m + n + 1\}$, $\{A_{2i}: 1 \leq i \leq n - 1\}$, $\{A_{2i}: n \leq i \leq m\}$, and $\{A_{-2i}: m + 1 \leq i \leq m + n + 1\}$. We have

From the above Table 7, $n_2(F_i) = M - n_1(F_i)$, where $F_i = H_{1i}$, O_{1i}, A_{1i}, P_i

$$n_2(F_i) = M - n_1(F_i) - |C|, \quad \text{where } F_i = H_{2i}, O_{2i}, A_{2i}$$

By symmetry, we have for $k = 1$, $n_k(A_{1i}) = n_k(A_{-1i})$, $n_k(O_{1i}) = n_k(O_{-1i})$, for $1 \leq i \leq m$ and $n_k(O_{2i}) = n_k(O_{-2i})$ for $1 \leq i \leq m$ and $n_k(A_{2i}) = n_k(A_{-2i})$ for $1 \leq i \leq m - 1$. For $m > n$, Define

$$X(G) = \sum_{i=1}^{2} X(H_{1i}) + \sum_{i=3}^{2m} X(H_{1i}) + X(H_{1(2m+1)}) + 2\sum_{i=1}^{n} X(O_{1i})$$
$$+ 2X(O_{1(n+1)}) + \sum_{i=n+2}^{m} X(O_{1i}) +$$
$$2\sum_{i=1}^{n} X(A_{1i}) + \sum_{i=n+1}^{m} X(A_{1i}) + \sum_{i=1}^{4m+2n+2} X(P_i) + \sum_{i=1}^{2m} X(H_{2i}) \quad .$$
$$+ 2\sum_{i=1}^{n} X(O_{2i}) + \sum_{i=n+1}^{m} X(O_{2i}) + 2\sum_{i=1}^{n-1} X(A_{2i}) +$$
$$\sum_{i=n}^{m} X(A_{2i}), \quad \text{where } X = WI_v, Sz_v, PI_v$$

Further, an analytical computation of $X(G)$ gives the result of the Theorem 4.2.

4.2. Degree-Based Topological Indices. This section analyzes some degree-based topological indices for the Hydrogen bonded boric acid 2D sheet lattice structure BAL-2D(m, n). A fundamental edge partition approach is proposed to derive various degree-based topological characteristics.

Two types of measurements are defined for each edge based on the degrees of end vertices, and they are given below[50]

$$a^+ = d(u) + d(v)$$
$$a^* = d(u)d(v)$$

Now, we define

$$\lambda(G) = \sum_{e=uv \in E(G)} \omega(p \circ q)^\alpha$$

where the various degree-based topological indices can be achieved by assigning appropriate values to λ, ω, α, p, and q and using mathematical operation $\circ$.

1. First Zagreb[51] $\lambda = M_1$, $p = a^+$, $q = 1$, $\omega = 1$, $\alpha = 1$, $\circ = \times$.
2. Second Zagreb[51] $\lambda = M_2$, $p = 1$, $q = a^*$, $\omega = 1$, $\alpha = 1$, $\circ = \times$.
3. Reduced second Zagreb[52] $\lambda = RM_2$, $p = a^+ - d(v) - 1$, $q = a^+ - d(u) - 1$, $\omega = 1$, $\alpha = 1$, $\circ = \times$.
4. Hyper Zagreb[53] $\lambda = HM$, $p = a^+$, $q = 1$, $\omega = 1$, $\alpha = 2$, $\circ = \times$.
5. Augmented Zagreb[54] $\lambda = AZ$, $p = \frac{1}{a^+ - 2}$, $\omega = 1$, $\alpha = 3$, $\circ = \times$.
6. Atom-bond connectivity[55] $\lambda = ABC$, $p = a^+ - 2$, $q = \frac{1}{a^*}$, $\omega = 1$, $\alpha = \frac{1}{2}$, $\circ = \times$.
7. Harmonic[56] $\lambda = H$, $p = \frac{1}{a^+}$, $q = 1$, $\omega = 2$, $\alpha = 1$, $\circ = \times$.
8. Sum-connectivity[57] $\lambda = SC$, $p = \frac{1}{a^+}$, $q = 1$, $\omega = 1$, $\alpha = \frac{1}{2}$, $\circ = \times$.
9. Geometric-arithmetic[58] $\lambda = GA$, $p = \frac{1}{a^+}$, $q = (a^*)^{1/2}$, $\omega = 2$, $\alpha = 1$, $\circ = \times$.

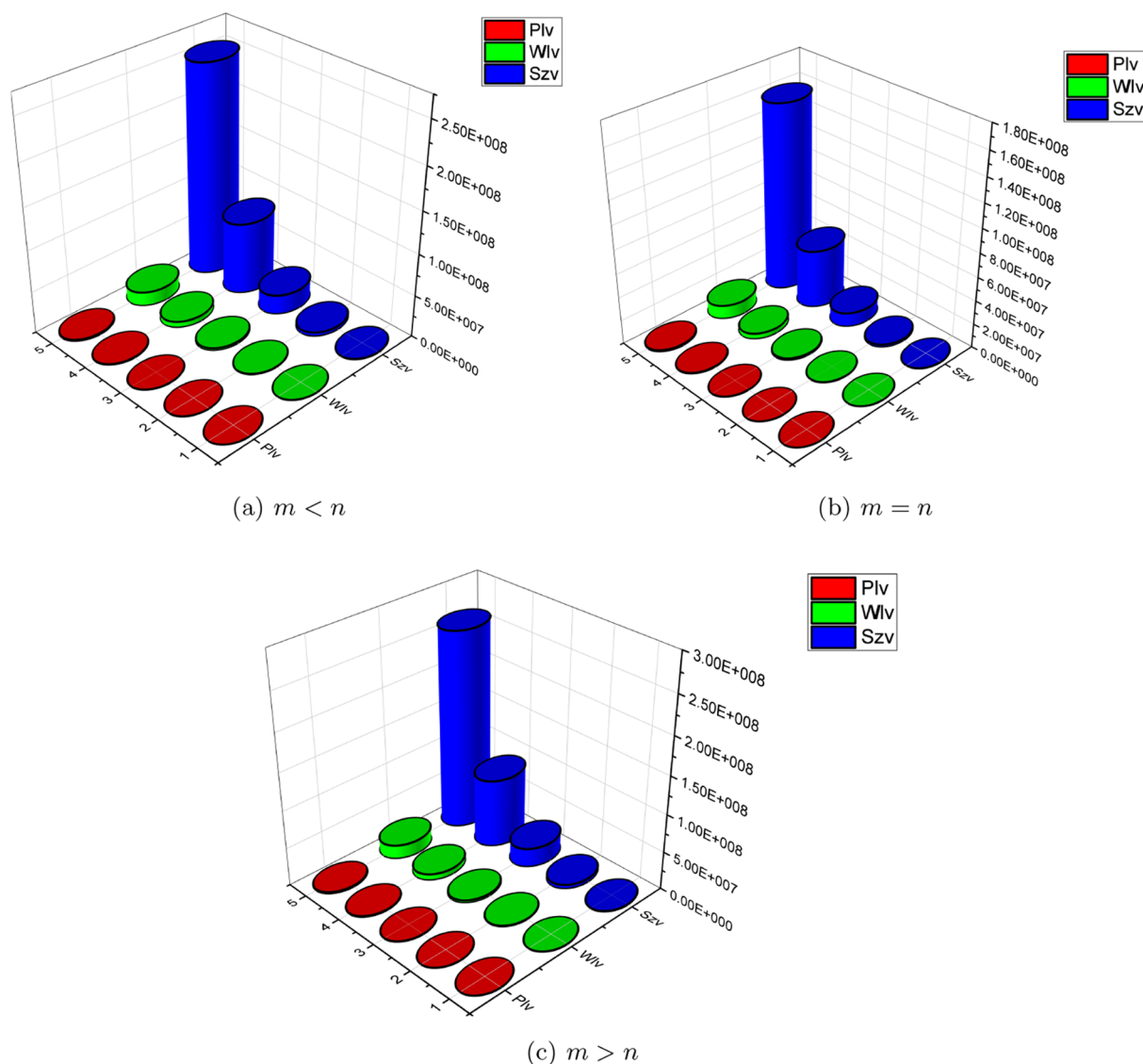(a) $m < n$

(b) $m = n$

(c) $m > n$

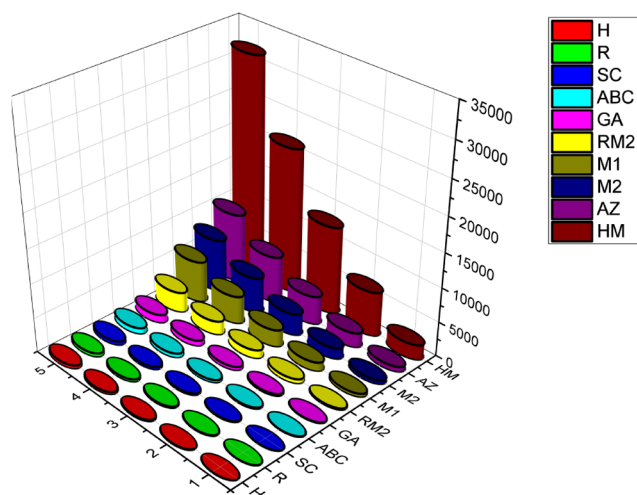**Figure 7.** Comparison of distance based indices values for boric acid 2D lattice.

Figure 8. Comparison of degree based indices values for boric acid 2D lattice

10. Randić[38] $\lambda = R$, $p = 1$, $q = \frac{1}{(a^*)^{1/2}}$, $\omega = 1$, $\alpha = 1$, $\circ = \times$.

Now, we have done the vertex degree-based edge set partition. The first edge set is divided into various classes according to the degree of each edge's end vertices to determine the degree-based indices. The ordered pairs of the degrees of the end vertices for the partitions are given in Table 8.

Theorem 4.3. Let G be a hydrogen bonded bulk boric acid 2D lattice sheet BAL-2D(m, n). Then

1. $M_1(G) = 160m + 80n + 192mn - 16$
2. $M_2(G) = 196m + 98n + 252mn - 28$
3. $RM_2(G) = 68m + 34n + 96mn - 14$
4. $HM(G) = 816m + 408n + 1032mn - 108$
5. $AZ(G) = \frac{1}{32}(8468m + 4234n + 10518mn - 1025)$
6. $ABC(G) = \frac{1}{3}(m(4\sqrt{2}\sqrt{3} + 30\sqrt{2} + 16)$
   $+ n(2\sqrt{2}\sqrt{3} + 15\sqrt{2} + 8) + 2\sqrt{2}\sqrt{3} - 3\sqrt{2}$
   $+ mn(36\sqrt{2} + 24) - 4)$
7. $H(G) = \frac{2}{15}(98m + 49n + 102mn - 2)$
8. $SC(G) = \frac{1}{15}(m(48\sqrt{5} + 20\sqrt{6} + 60) - 5\sqrt{6} - 12\sqrt{5}$
   $+ n(24\sqrt{5} + 10\sqrt{6} + 30) + mn(72\sqrt{5} + 30\sqrt{6})$
   $+ 30)$

9. $GA(G) = \frac{1}{5}(5\sqrt{3} - 8\sqrt{6} + m(10\sqrt{3} + 32\sqrt{6} + 60)$
$+ n(5\sqrt{3} + 16\sqrt{6} + 30) + mn(48\sqrt{6} + 60))$

10. $R(G) = \frac{1}{3}(2\sqrt{3} - 2\sqrt{6} + m(4\sqrt{3} + 8\sqrt{6} + 14)$
$+ n(2\sqrt{3} + 4\sqrt{6} + 7) + mn(12\sqrt{6} + 12) + 1)$

4.3. Numerical Values. In this section, we provide numerical values of distance and degree-based indices for $1 \leq m, n \leq 6$ in Tables 9 and 10 and Figures 7 and 8 show that Szeged index has largest values while PI index has the least values. The generated topological descriptors were plotted using the Orgin 2020b for a graphical comparison.

5. CONCLUSIONS

In this study, we used the cut method to develop a perfect technique for determining the value of a hydrogen-bonded 2D lattice of boric acid using the vertex-version of distance and degree-based descriptors. Chemists can anticipate a range of molecular compound properties using these indices instead of expensive or time-consuming testing. It is simple to see as numeric values for a complex structure. Additionally, we checked the results from the literature on the topological index using the vertex-based indices technique.[59] We examine the quantitative measure of distance and degree-based indices in Figures 7 and 8. We can see that Szeged and hyper Zagreb indices have the highest numerical values on the initial structure than other indices. These computational analyses are extremely useful in determining specific applications, such as the physicochemical properties of the boric acid structure. From this study, we believe that our results will help to predict NMR patterns through further analysis. In the same way, it would be helpful for the researchers to get novel results in theoretical and experimental spectroscopic studies.[60−62]

■ AUTHOR INFORMATION

Corresponding Author

Roy Santiago − *Department of Mathematics, Vellore Institute of Technology, Vellore 632 014, India;* ⊙ orcid.org/0000-0002-5542-6581; Email: roy.santiago@vit.ac.in

Author

Sahaya Vijay Jeyaraj − *Department of Mathematics, Vellore Institute of Technology, Vellore 632 014, India*

Complete contact information is available at:
https://pubs.acs.org/10.1021/acsomega.3c02477

Author Contributions

J.S.: Data collection, writing of an original draft preparation, visualization, software, methodology and investigation. S.R.: Conceptualization, supervision, validation, investigation, writing, reviewing, and editing.

Notes

The authors declare no competing financial interest.

■ REFERENCES

(1) Azeem, M.; Jamil, M. K.; Shang, Y. Notes on the localization of generalized hexagonal cellular networks. *Mathematics* **2023**, *11* (4), 844.

(2) Jolly, W. L. *Modern Inorganic Chemistry*, 2nd ed.; MacGraw-Hill: New York, 1991; p 635.

(3) Housecroft, C. E., Sharpe, A. G. *Inorganic Chemistry*, 2nd ed.; Pearson/Prentice Hall: Hoboken, NJ, 2005; p 905.

(4) Cohen, P.; Graves, H. W. Chemical shim control for power reactors. *Nucleonics* **1964**, *22* (5), 75−82.

(5) Myerscough, P.B. *Nuclear Power Generation (Third ed.) Incorporating Modern Power System Practice*; British Electricity International; 1992, pp 1−110.

(6) Hargraves, R.; Moir, R. Liquid fluoride thorium reactors: An old idea in nuclear power gets reexamined. *Am. Sci.* **2010**, *98* (4), 304−313.

(7) https://www.chemzipper.com/2020/10/why-boric-acid-exist-in-solid-state.html?m=0.

(8) Arockiaraj, M.; Clement, J.; Balasubramanian, K. Topological indices and their application to circumcised donut benzonoid systems, kekulenes and drugs. *Polcycl. Aromat. comp.* **2020**, *40*, 280−303.

(9) Imran, M.; Baig, A. Q.; Ali, H. On molecular topological properties of hex-derived networks. *J. Chemom* **2016**, *30*, 121−129.

(10) Dias, J. R. A periodic table for polycyclic aromatic hydrocarbons. Isomer enumeration of fused polycyclic aromatic hydrocarbons. Part I. *J. Chem. Inf. Comput. Sci.* **1984**, *24*, 124−135.

(11) Todeschini, R.; Consonni, V. *Molecular Descriptors for Chemo-informatics*; Wiley-VCH: Weinheim, 2009.

(12) Gutman, I.; Cyvin, S.J. *Introduction to the Theory of Benzenoid Hydrocarbons*; Springer-Verlag: Berlin, 1989.

(13) Balasubramanian, K.; Kaufman, J. J.; Koski, W. S.; Balaban, A. T. Graph theoretical characterization and computer-generation of certain carcinogenic benzenoid hydrocarbons and identification of bay regions. *J. Comput. Chem.* **1980**, *1* (2), 149−157.

(14) Basak, S. C.; Mills, D.; Mumtaz, M. M. Quantitative structure-activity relationship (QSAR) study of dermal absorption using theoretical molecular descriptors. *SAR QSAR Environ. Res.* **2007**, *18*, 45−55.

(15) Imran, M.; Hayat, S. On counting polynomials of certain polyomino chains. *Bulg. Chem. Commun.* **2016**, *48*, 332−337.

(16) Azeem, M.; Nadeem, M. F. Metric-based resolvability of polycyclic aromatic hydrocarbons. *Eur. Phys. J. Plus* **2021**, *136* (4), 1−14.

(17) Imran, M.; Hayat, S.; Shafiq, M. K. Computing omega and Sadhana polynomials of carbon nanotubes. *Optoelectron. Adv. Mater. Rapid Commun.* **2014**, *8* (11−12), 1218−1224.

(18) Azeem, M.; Imran, M.; Nadeem, M. F. Sharp bounds on partition dimension of hexagonal Möbius ladder. *J. King Saud Univ Sci.* **2022**, *34* (2), 101779.

(19) Gute, B.; Grunwald, G.; Basak, S. C. Prediction of the dermal and penetration of polycyclic aromatics: a hierachical QSAR approach. *SAR QSAR Environ. Res.* **1999**, *10*, 1−15.

(20) Viswanadhan, V. N.; Mueller, G. A.; Basak, S. C.; Weinstein, J. N. Comparison of a neural net-based QSAR algorithm (PCANN) with hologram-and multiple linear regression-based QSAR approaches: application to 1,4-dihydropyridine-based calcium channel antagonists. *J. Chem. Inf. Comput. Sci.* **2001**, *41* (3), 505−511.

(21) Korinth, G.; Wellner, T.; Schaller, K. H.; Drexler, H. Potential of the octanol-water partition coefficient (logP) to predict the dermal penetration behaviour of amphiphilic compounds in aqueous solutions. *Toxicol. Lett.* **2012**, *215* (1), 49−53.

(22) Williams, A. C.; Barry, B. W. Terpenes and the lipid-protein-partitioning theory of skin penetration enhancement. *Pharm. Res.* **1991**, *8* (1), 17−24.

(23) Roberts, M.S.; Walters, K.A. Dermal absorption and toxicity assessment. *New York: Drugs and the Pharamaceutical Sciences*; Informa Healthcare Inc. , 2008.

(24) Liu, J. B.; Arockiaraj, M.; Arulperumjothi, M.; Prabhu, S. Distance based and bond additive topological indices of certain

repurposed antiviral drug compounds tested for treating COVID-19. *Int. J. Quantum Chem.* **2021**, *121* (10), 26617.

(25) Hayat, S.; Khan, S.; Khan, A.; Imran, M., et al. Distance-based topological descriptors for measuring the π-electronic energy of benzenoid hydrocarbons with applications to carbon nanotubes. *Math. Methods Appl. Sci.* **2020** DOI: 10.1002/mma.6668.

(26) Malik, M. Y. H.; Binyamin, M. A.; Hayat, S. Correlation ability of degree-based topological indices for physicochemical properties of polycyclic aromatic hydrocarbons with applications. *Polycycl. Aromat. Compd.* **2022**, *42* (9), 6267−6281.

(27) Brezovnik, S.; Tratnik, N. General cut method for computing Szeged-like topological indices with applications to molecular graphs. *Int. J. Quantum Chem.* **2021**, *121* (6), 26530.

(28) Zhang, X.; et al. Edge-version atom-bond connectivity and geometric arithmetic indices of generalized bridge molecular graphs. *Symmetry* **2018**, *10* (12), 751.

(29) Zhang, X.; Awais, H. M.; Javaid, M.; Siddiqui, M. K.; et al. Multiplicative Zagreb indices of molecular graphs. *J. Chem.* **2019**, *2019*, 1−19.

(30) Zhang, X.; et al. On degree based topological properties of two carbon nanotubes. *Polycycl. Aromat. Compd.* **2022**, *42* (3), 866−884.

(31) Devillers, J.; Balaban, A.T. *Topological Indices and Related Descriptors in QSAR and QSPR*; Gordon and Breach: Amsterdam, 1999.

(32) Hayat, S.; Imran, M. Computation of topological indices of certain networks. *Appl. Math. Comput.* **2014**, *240*, 213−228.

(33) Baig, A. Q.; Imran, M.; Ali, H. Computing omega, sadhana and PI polynomials of benzoid carbon nanotubes. *Optoelectron. Adv. Mater. Rapid Commun.* **2015**, *9*, 248−255.

(34) Furtula, B.; Gutman, I. Relation between second and third geometric-arithmetic indices of trees. *J. Chemom.* **2011**, *25*, 87−91.

(35) Hayat, S.; Imran, M. Computation of certain topological indices of nanotubes. *J. Comput. Theor. Nanosci.* **2015**, *12*, 70−76.

(36) Khadikar, P.; Karmarkar, S.; Agrawal, V.; Singh, J.; Shrivastava, A.; Lukovits, I.; Diudea, M.; et al. Szeged index-applications for drug modeling. *Lett. Drug Design Discov* **2005**, *2*, 606−624.

(37) Wiener, H. Structural determination of paraffin boiling points. *J. Am. Chem. Soc.* **1947**, *69*, 17−20.

(38) Randić, M. On characterization of molecular branching. *J. Am. Chem. Soc.* **1975**, *97*, 6609−6615.

(39) Han, J.; Yau, C. W.; Lam, C. K.; Mak, T. C. W. Designed supramolecular assembly of hydrogen-bonded anionic rosette layers. *J. Am. Chem. Soc.* **2008**, *130* (31), 10315−26.

(40) da Silva, M. B.; dos Santos, R. C. R.; da Cunha, A. M.; Valentini, A.; Pessoa, O. D. L.; Caetano, E. W. S.; Freire, V. N. Structural, electronic, and optical properties of bulk boric acid 2A and 3T polymorphs: Experiment and density functional theory calculations. *Cryst. Growth Des.* **2016**, *16* (11), 6631−6640.

(41) Klavžar, S.; Gutman, I.; Mohar, B. Labelling of benzenoid systems which reflects the vertex-distance relation. *J. Chem. Inf. Comput. Sci.* **1995**, *35*, 590−593.

(42) Djoković, D. Distance preserving sub graphs of hyper cubes. *J. Comb. Theory* **1973**, *14*, 263−7.

(43) Zhang, X.; Jiang, H.; Liu, J. B.; Shao, Z. The cartesian product and join graphs on edge-version atom-bond connectivity and geometric arithmetic indices. *Molecules* **2018**, *23* (7), 1−17.

(44) Zhang, X.; et al. Study of Hardness of Superhard Crystals by Topological Indices. *J. Chem.* **2021**, *10*, 7−20.

(45) Zhang, X.; Siddiqui, M. K.; Javed, S.; Sherin, L.; Kausar, F.; Muhammad, M. H. Physical analysis of heat for formation and entropy of Ceria Oxide using topological indices. *Journal. Comb Chem. High Throughput Screen.* **2022**, *25* (3), 441−450.

(46) Winkler, P. Isometric embeddings in products of complete graphs. *Discret. Appl. Math.* **1984**, *7*, 221−5.

(47) Gutman, I. Selected properties of the Schultz molecular topological index. *J. Chem. Inf. Comput. Sci.* **1994**, *34*, 1087−1089.

(48) Khadikar, P. V.; Karmarkar, S.; Agrawal, V. K. A novel PI index and its applications to QSPR/QSAR studies. *J. Chem. Inf. Comput. Sci.* **2001**, *41*, 934−949.

(49) Arockiaraj, M.; Clement, J.; Balasubramanian, K. Analytical expressions for topological properties of polycyclic benzenoid networks. *J. Chemom.* **2016**, *30*, 682−697.

(50) Arockiaraj, M.; Paul, D.; Klavžar, S.; Clement, J.; Tigga, S.; Balasubramanian, K. Relativistic distance based and bond additive topological descriptors of Zeolite Rho materials. *J. Mol. Struct.* **2022**, *1250*, 131798.

(51) Gutman, I.; Trinajstić, N. Graph theory andmolecular orbitals. Total π-electron energy of alternant hydrocarbons. *Chem. Phys. Lett.* **1972**, *17*, 535−538.

(52) Furtula, B.; Gutman, I.; Ediz, S. On difference of Zagreb indices. *Disc. Appl. Math.* **2014**, *178*, 83−88.

(53) Shirdel, G. H.; Rezapour, H.; Sayadi, A. M. The hyper-Zagreb index of graph operations. *Iran. J. Math. Chem.* **2013**, *4* (2), 213−220.

(54) Furtula, B.; Graovac, A.; Vukičević, D. Augmented Zagreb index. *J. Math. Chem.* **2010**, *48* (2), 370−380.

(55) Estrada, E.; Torres, L.; Rodríguez, L.; Gutman, I. An atom-bond connectivity index: modelling the enthalpy of formation of alkanes. *Indian J. Chem.* **1998**, *37A*, 849−855.

(56) Fajtlowicz, S. On conjectures of Graffiti-II. *Congr. Numer.* **1987**, *60*, 187−197.

(57) Zhou, B.; Trinajstić, N. On a novel connectivity index. *J. Math. Chem.* **2009**, *46* (4), 1252−1270.

(58) Vukičević, D.; Furtula, B. Topological index based on the ratios of geometrical and arithmetical means of end-vertex degrees of edges. *J. Math. Chem.* **2009**, *46*, 1369−1376.

(59) Azeem, M.; et al. Verification of some topological indices of Y-junction based nanostructures by M-polynomials. *J. Math.* **2022**, *2022*, 1−18.

(60) Balasubramanian, K. Operator and algebraic methods for NMR spectroscopy. I. Generation of NMR spin species. *J. Chem. Phys.* **1983**, *78* (11), 6358−6368.

(61) Balasubramanian, K. Topological and group theoretical analysis in dynamic NMR spectroscopy. *J. Phys. Chem.* **1982**, *86* (24), 4668−4674.

(62) Raza, Z.; Arockiaraj, M.; Maaran, A.; Kavitha, S. R. J.; Balasubramanian, K. Topological entropy characterization, NMR and ESR spectral patterns of coronene-based transition metal organic frameworks. *ACS Omega* **2023**, *8*, 13371.